Effects of Knock Intensity Measurement Technique and Fuel Chemical Composition on the Research Octane Number (RON) of FACE Gasolines: Part 1 - Lambda and Knock Characterization

Alexander Hoth, Christopher P. Kolodziej

Argonne National Laboratory, 9700 S. Cass Avenue, Lemont, IL 60439, USA

Abstract:

The Research and Motor Octane Number (RON and MON) rate the knock propensity of gasoline in the Cooperative Fuel Research (CFR) engine by comparing the knock intensity of sample fuels relative to that of primary reference fuels (PRF), a binary blend of iso-octane and n-heptane. Important differences exist between standard octane testing and automotive spark ignition (SI) engine knock testing including speed, load, air-to-fuel equivalence ratio (lambda), and knock characterization, which lead to a discrepancy between a fuel's RON rating and its knock resistance characterized on an automotive SI engine based on knock-limited spark advance. This is the first of a set of three publications which modify operating parameters of the RON test method (ASTM D2699) to investigate the effects of these differences with automotive SI engine knock-limited spark advance testing. A fuel's standard RON is evaluated at the lambda of the highest knock intensity, whereas automotive SI engines typically operate at stoichiometry. This study analyzes the effects of a stoichiometric RON rating methodology. Additionally, the knock

intensity response from the standard CFR knockmeter system is compared to a cylinder pressure oscillation-based knock intensity at several lambda settings. All experiments were performed with a set of seven Coordinating Research Council (CRC) Fuels for Advanced Combustion Engines (FACE) gasolines with approximately 95 RON. The fuel chemical composition impacted the lambda of the highest knock intensity, which resulted in fuel-specific offsets between the standard and stoichiometric RON ratings. The knock system comparison showed significant offsets between cylinder pressure-based and knockmeter-based knock intensity levels.

1. Introduction

The performance and efficiency of spark ignition (SI) engines are limited by knocking combustion, an abnormal combustion phenomenon which can lead to potentially damaging high-frequency pressure oscillations within the combustion chamber. Knocking combustion is dependent on four major parameters: geometric engine design, operating conditions, charge preparation, and fuel properties [1]. The engine design affects the tendency for knock through the level of compression (compression ratio), the turbulence level via the design of the intake port, the recirculated exhaust gas fraction in the combustion chamber and the combustion chamber dimensions (such as bore). Operating conditions and combustion processes such as engine speed, engine load, spark timing, and air-to-fuel equivalence ratio (lambda) additionally influence the tendency for knock in SI engines. Furthermore, fuel chemical composition affects the tendency for knock.

Fuel characteristics are regulated worldwide by governments referencing standards such as ASTM D4814, EN228, JIS K 2202, and others [2 - 4]. The research octane number (RON) and motor octane number (MON) test methods characterize the knock propensity of gasoline based on the standardized methods, D2699

(RON) and D2700 (MON), established by ASTM International [5 - 6]. The octane numbers are assessed in the standardized Cooperative Fuel Research (CFR) engine by comparing the knock intensity of the sample fuel to the knock intensity of primary reference fuels (PRFs). The octane number of PRFs are defined as the volumetric concentration of iso-octane in a binary blend with n-heptane [5 - 6].

The CFR engine geometry and operating conditions of the test methods were established by the Cooperative Fuel Research committee in the 1930s, which was later superseded by the Coordinating Research Council (CRC) [7]. Some of the differences in the test parameters between the RON conditions and automotive engine knock testing are listed in Table 1, including: the method of evaluating knock intensity, lambda, spark timing, and the compression ratio (fixed vs. variable). Modern commercial SI engines usually operate at stoichiometry due to the air-to-fuel equivalence ratio requirements of a three-way catalyst for successful exhaust aftertreatment [1].

Yates et al. estimated the in-cylinder pressure-temperature (P-T) trajectories of the RON and MON tests and how automotive engine technologies, such as boosting and direct injection, generally shift the P-T trajectory “beyond RON” towards higher cylinder pressure for a given cylinder temperature [8]. Kalghatgi proposed the Octane Index, which uses RON, MON, and an engine operation-specific K to interpolate, or extrapolate, the knock resistance of a fuel at a given set of conditions [9]. Equation 1 presents the Kalghatgi Octane Index calculation, where RON conditions are represented by K = 0 and MON by K = 1. The Antiknock Index (AKI) can be calculated with a K value of 0.5 and typically represents historical (1950s) engine operation [10]. Studies have shown that boosted SI engines can achieve negative K values which leads to an increased knock resistance for fuels with higher octane sensitivity (RON-MON) [9 - 11]. According to Mittal and Heywood, automotive engines as of 2009 show a range of K from -0.6 to 0.2 depending on the operating conditions [10]. With the increased popularity of direct injection and boosting, this range is expected to further shift negative.

$$OI = RON - K * (RON - MON) \quad \text{(Eq. 1) [9]}$$

Table 1. Overview of the differences in operating conditions between the ASTM RON test method and knock-limited spark advance (KLSA) type testing utilized on automotive SI engines. [5]

Parameter	RON Rating	KLSA type testing
Knock Intensity	CFR knockmeter system	Cylinder pressure oscillations
Lambda	Peak knockmeter reading	Generally stoichiometric
Spark Timing	Constant at 13°bTDC	Limited by incipient knock
Compression Ratio	Variable, depending on RON	Fixed / Interchangeable

In an experimental study, Mittal and Heywood found K to depend on lambda, engine speed, intake temperature, and intake pressure. The compression ratio and spark plug location were found to have a reduced impact. As a result, Mittal and Heywood suggested updating the RON and MON operating conditions towards higher engine speeds and boost pressures while slightly reducing the intake air temperature [12].

Other studies analyzed the chemical and physical effects on the octane number of added ethanol. Hunwartzen proposed to utilize a variable needle jet to account for ethanol's lower stoichiometric air-to-fuel ratio [13]. Foong et al. showed in their experimental study that added ethanol significantly reduces the mixture temperature during the RON test and might lead to a saturated fuel-air mixture in the intake port. Therefore, Foong et al. proposed to maintain a steady mixture temperature while increasing the intake air temperature accordingly. This modified RON test method reduced the RON ratings of fuels inversely proportionate to their heat of vaporization (HOV) [14]. To note, three of the sample fuels utilized in the current study have an ethanol concentration of 15 percent by volume, which limits the described charge cooling artifact effects.

A recent study by Hauber et al. proposed significant updates to the RON test method as well as hardware changes to the CFR engine. Their "gasoline knock index" rates a fuel by the critical compression ratio necessary to reach a cylinder pressure transducer-based knock intensity threshold under stoichiometric conditions. The authors showed good correlations between the gasoline knock index and RON [15].

This study analyzes the sole effect of changes in the lambda without adapting other engine operating conditions of the RON testing procedure. The knock intensity response to changes in lambda will be analyzed for full boiling range gasolines with varying chemical composition. In addition, differences in the knock intensity assessment method and their effect on the RON calculation are investigated. This is the first part of a three-part journal article series that analyzes the effects of the first and second parameters of Table 1. The differences in spark timing and compression ratio between RON rating and KLSA-type testing outlined in rows three and four of Table 1 will be covered in the following two parts of the publication series.

2. Experimental Configuration

2.1. Engine Setup

The experimental study was conducted on a standard, naturally aspirated, carbureted CFR F1 engine, which was instrumented with a host of common engine combustion research analysis tools. However, no modifications to the intake, exhaust, or combustion chamber geometry were made to maintain full compliance with the ASTM D2699 RON rating procedure. Table 2 contains an overview of the additionally installed measurement equipment, which allowed for a better characterization of the engine operating conditions and combustion behavior during the RON rating procedure. In addition, all critical

temperatures, pressures, and the knockmeter response were captured through the installed LabVIEW data acquisition system. Furthermore, high-speed crank angle-based measurements of the intake, exhaust, and cylinder pressures were captured with an AVL IndiMicro system. An AVL GU13Z-24 flush-mounted spark plug pressure transducer was used to avoid additional modifications to the cylinder head which could influence the combustion or heat transfer behavior. Prior to using the indicating spark plug, a "Fit for Use" test (following ASTM D2699) was performed with the standard Champion D16 spark plug and compared to the AVL indicating spark plug, but no impact on the knockmeter knock intensities of the reference and standardization fuels were noticed. Common concerns about spark plug pressure transducers exist and are addressed in *Section 3.2. Pressure-Based Knock Intensity*.

Table 2. Combustion research measurement and instrumentation systems employed on the Argonne CFR engine.

Crankshaft angle-based measurements	
Crank-angle based DAQ	AVL IndiMicro & crankshaft encoder
Spark timing	Current clamp on coil wire
Intake pressure	Flush-mounted Kulite ETL-189-190M-2.5bara (0.2 crank-angle resolution)
Exhaust pressure	Flush-mounted Kulite EWCTV-312M-3.5bara (0.2 crank-angle resolution)
Cylinder pressure	AVL GU13Z-24 flush-mounted spark plug pressure transducer (0.1 crank angle resolution)
Time-based measurements	
Time-based DAQ	LabVIEW
Intake pressure	Setra 3550 pressure transducer
Exhaust pressure	Setra 3550 pressure transducer
Intake, mixture, exhaust, coolant, and oil temperature	K-type thermocouples
Fuel rate	Emerson CMF010M Coriolis Meter
Lambda	Bosch wide-band lambda sensor LSU 4.9
CFR knock units	Data-logged knockmeter signal

2.2. Testing Procedures

The RON rating procedure is defined by the ASTM D2699 test standard, which provides the applicable operating conditions for the CFR engine. This includes an engine speed of 600 rpm, an intake air

temperature and compression ratio dependent on the barometric pressure, and other operation parameters previously specified in Table 1. Certain engine standardization tests are required before rating the RON of a sample fuel. These tests include a motoring peak pressure test to evaluate the achieved compression pressure and a knocking "Fit for Use" test. The "Fit for Use" test requires using PRFs to rate the octane number of Toluene Standardization Fuels (TSF) within a given tolerance. If a TSF is rated outside its tolerance, the intake air temperature has to be tuned accordingly until the octane number rating matches the specifications of ASTM D2699. For this testing, a fully compliant CFR RON rating engine was used without the need for intake air temperature tuning. The intake air temperature was solely adjusted based on the barometric pressure during testing [5].

This study was performed using "Procedure A: Bracketing – Equilibrium Fuel Level", for which the engine was operated at the lambda of highest knock intensity and a compression ratio that is prescribed based on the expected octane level of the sample fuel. The standard RON of the sample fuel was then calculated based on an interpolation between the knock intensity of the sample fuel relative to the PRFs, Equation 2. Table 3 contains an overview of the used acronyms.

$$ON_S = ON_{LRF} + \left(\frac{KI_{LRF} - KI_S}{KI_{LRF} - KI_{HRF}}\right) * (ON_{HRF} - ON_{LRF}) \quad \text{(Eq. 2) [5]}$$

Table 3. Parameters for interpolating the Octane Number using Equation 2 [5].

Parameter	Description
ON_S	Octane number of the sample fuel
ON_{LRF}	Defined octane number of the low PRF
ON_{HRF}	Defined octane number of the high PRF
KI_S	Knockmeter reading of the sample fuel
KI_{LRF}	Knockmeter reading of the low PRF
KI_{HRF}	Knockmeter reading of the high PRF

The lambda of the highest knock intensity is neither measured nor recorded in a standard RON test. For this study, the lambda was measured by a Bosch LSU 4.9 wide-band lambda sensor. Each fuel has a unique peak knocking lambda (PKL) which is affected by the fuel composition and is typically slightly rich (0.88-0.95 lambda) for most fuels [16, 17]. It is important to point out that the RON test method rates the octane number of a fuel at its PKL, while automotive spark-ignition engines operate mostly at stoichiometry. During the course of this study, a wide sweep of lambda from 0.8 to 1.0 was performed for each fuel, with increments of 0.02 lambda near the fuel's PKL. At each lambda, the engine was allowed to reach steady-state conditions before recording the data point. The most interesting lambda values were that of peak knock and at stoichiometric operation. Those points allowed for a comparison between the knock propensity of the fuels at their RON rating conditions and at stoichiometry, which is how these fuels are most often operated in automotive SI engines [1].

2.3. Fuel Overview

Seven fuels for advanced combustion engines (FACE) supplied by the Coordinating Research Council (CRC) were selected for this testing, Table 4. The seven FACE gasolines chosen for this study have a RON rating of approximately 95 ± 1.5, but vary in chemical composition. The differences in chemical composition affect the fuel's PKL, as well as their detailed knocking characteristics as measured by a cylinder pressure transducer.

In this study, the FACE gasolines were first categorized by their chemical classes to be mainly aromatic or iso-paraffinic. Each of the groups was further characterized by the concentration of ethanol, olefins, or cyclo-paraffins, Figure 1. The chemical composition of FACE gasolines D, F, G, and H+E15 fall within the typical composition range of market gasoline. [18, 19]. The FACE gasolines A, C, and H originally have a RON below 95, but a previous CRC report outlined that 15 vol% of ethanol increased the RON to around 95. Throughout previous CRC reports, these gasolines were thoroughly characterized in

experimental engines and combustion facilities, such as rapid compression machines [20]. Differences in combustion and knocking behavior can be associated with differences in the chemical hydrocarbon composition of the fuels.

Table 4. Fuel overview with physical properties and chemical composition.

O – Olefin, cP – Cyclo-Paraffinic, E15 – 15 vol% Ethanol [20]

FACE Fuel	RON	MON	S	T90 (°F)	Iso-paraffin (vol%)	Aromatic (vol%)	N-Paraffin (vol%)	Cyclo-Paraffin (vol%)	Olefin (vol%)	Categorization	Symbol
B	95.8	92.4	3.4	236	86.9	5.8	8.0	0.1	0.02	Iso-paraffinic	
D	94.2	87.0	7.2	331	42.1	33.4	24.1	0.1	0.04	Aromatic	
F	94.0	88.1	5.9	242	67.6	7.7	4.4	11.0	9.4	Iso-paraffinic, O, cP	
G	96.5	85.8	10.7	343	38.4	33.6	6.7	11.5	8.1	Aromatic, O, cP	
A + E15	94.8	89.4	5.4	219	73.1	0.3	9.9	1.4	0.2	Iso-paraffinic, E15	
C + E15	94.8	88.8	6.0	241	59.3	3.3	20.8	0.3	1.1	Iso-paraffinic, E15	
H + E15	94.1	83.3	10.8	323	19.4	30.4	19.1	8.9	5.8	Aromatic, O, cP, E15	

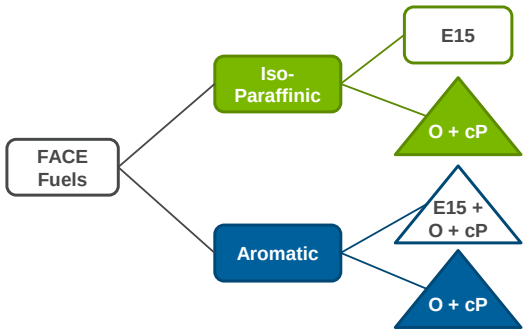

Figure 1. Fuel characterization methodology and legend symbols with O+cP as an abbreviation for Olefin and Cyclo-Paraffin and E15 for 15 vol% Ethanol.

In addition, PRF97, PRF95, and PRF93 were used as reference fuels to bracket the knock intensity of the seven FACE gasolines. The PRFs are binary blends of iso-octane and n-heptane with the RON number being

equivalent to the volumetric fraction of iso-octane. Following the analogy from Table 4, these PRFs would be classified as highly iso-paraffinic.

Furthermore, the respective Toluene Standardization Fuels (TSF) were used at RON 96.9 and RON 93.4 levels. These tertiary blends of toluene, n-heptane, and iso-octane serve to validate the engine compliance with the ASTM test procedure, but in this study also serve as highly aromatic test fuels. The exact compositions are shown in Table 5 [5].

Table 5. Compositions of tested ASTM Toluene Standardization Fuels [5].

TSF RON Level	Toluene [vol%]	n-Heptane [vol%]	iso-Octane [vol%]
93.4	74	26	0
96.9	74	21	5

3. Knock Intensity Assessment

The octane ratings of a sample fuel are calculated based on the knock intensity of the sample fuel relative to the knock intensity of high and low bracketing PRFs (Equation 2). This study focused on two different knock intensity characterization methods: the standard CFR knockmeter system and a cylinder pressure transducer-based knock intensity method comparable to what is used on research automotive SI engines.

3.1. CFR Knockmeter System

The knock detection in the standard CFR engine is accomplished through the knockmeter system specified by the ASTM D2699 method and the CFR manual [5, 21]. This system consists of three main components;

a sensor, a signal conditioning unit, and a knock intensity display. The D1 pickup sensor is directly mounted in a cavity of the combustion chamber. The CFR engine manual states that the D1 pickup measures the deflection of the membrane and gives a voltage proportional to the first derivative of the cylinder pressure [21]. In the next step, the signal is conditioned in the 501C Detonation Meter. Studies have found that the detonation meter filters the input signal coming from the D1 pickup and attenuates the high-frequency pressure oscillations [7, 22 - 24].

Figure 2 shows a comparison of a crank angle resolved cylinder pressure trace and the 501C detonation meter filtered input signal. The cylinder pressure trace clearly shows high-frequency pressure oscillations associated with knocking combustion. However, the input signal to the 501C Detonation Meter shows no such oscillations. A recent study by Swarts et al. showed that the D1-pickup (knock sensor) can pick up pressure oscillations but previous studies by Hauber et al. and Swarts et al. showed, that an R-C Filter in the input of the 501C Detonation Meter filters out most of the oscillations that were captured by the D1 pickup [7, 22 -25]. After signal conditioning, the output voltage is routed to a knockmeter scale which displays the knock intensity in a range from 0 to 100. The 501C detonation meter allows for easy adjustments of the filter settings to set the knock intensity appropriately [7, 21, 24]. Rockstroh et al. showed three widely different cylinder pressure traces while maintaining a constant knockmeter knock intensity [26].

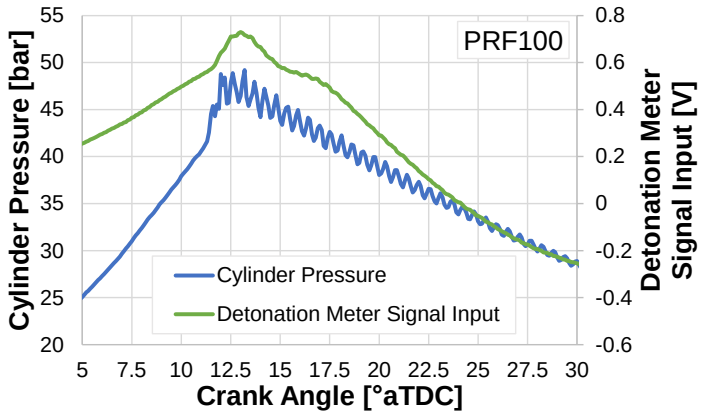

Figure 2. Crank-angle resolved 501C detonation meter input signal and cylinder pressure trace vs. crank angle.

3.2. Pressure-Based Knock Intensity

An indicating spark plug was used to capture the cylinder pressure, simultaneous to performing the standard RON measurements with the CFR knockmeter D1 pickup installed, at a sampling frequency of one sample per 0.1 CAD (36 kHz for 600 rpm). Knocking combustion is associated with high-frequency pressure oscillations during the combustion event. A study by Rockstroh et al. found the dominant knock frequencies in the CFR engine to occur at 6, 10, and 14 kHz, with two orders of magnitude more energy occurring at 6 kHz than the other two frequencies [26].

In addition to the standard knockmeter system knock intensity, the maximum amplitude of pressure oscillations (MAPO) was used as a cylinder pressure transducer-based knock intensity. A 4 kHz to 18 kHz bandpass filter was applied to the cylinder pressure to extract knock relevant frequencies up to the Nyquist frequency. A window from -60 to +60 °aTDC was used to prevent undesirable influences from valve events. In the next step, the filtered pressure signal was rectified and the maximum amplitude of pressure oscillations (MAPO) was identified for each cycle. Finally, the MAPO value of each cycle was averaged over the measurement duration of 300 cycles. Figure 3 shows a comparison of the unfiltered

cylinder pressure trace (blue) with an overlaid 4 kHz low pass filtered cylinder pressure trace (black) and bandpass filtered pressure oscillations on a crank angle basis (orange) [16].

The knockpoint describes a characteristic inflection point in the cylinder pressure trace leading to a strong pressure rise due to autoignition [7]. The knockpoint is displayed as a brown square in Figure 3. Before knockpoint, no significant pressure fluctuations can be observed. As a result, the cylinder pressure trace and the low pass filtered cylinder pressure trace are identical. After rectification, the bandpass filtered pressure trace (orange) should reach a zero level before again reaching a local peak amplitude. Figure 3 shows a noticeable offset of the lowest MAPO from the zero level. This is due to the sampling rate of 36 kHz, which is the upper limit of the crank angle resolved sampling frequency. The offset at the highest amplitude of the band-pass filtered pressure is of most interest as it is used to compute MAPO.

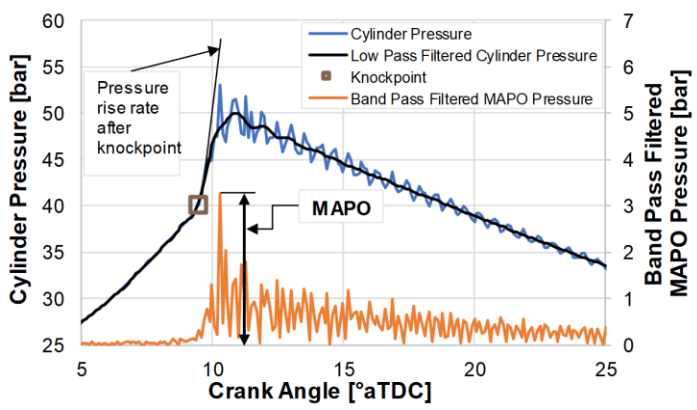

Figure 3. Comparison of crank angle-resolved, representative cylinder pressure, and applied filters for calculating MAPO [16].

The utilized AVL GU13Z-24 pressure sensor has a natural frequency of 115 kHz and the indicating system allowed for a time-based sampling frequency of 100 kHz. A standard RON test for PRF 98 was recorded at 100 kHz sampling rate and analyzed with two different filter cut off frequencies. Of the 300 cycles captured, the average and standard deviation of MAPO for two different cut-off frequencies are shown in Table 6. First, a filter cut off frequency of 18 kHz was used to represent the Nyquist frequency of the standard 36 kHz crank angle-based sampling rate. Second, for the 100 kHz time-based sampled data, a

40 kHz frequency cut-off was used according to Shalari and Ghandhi who suggested a maximum cut-off frequency at 40 kHz to prevent potential artificial pressure influence originating from the natural frequency of the pressure transducer [27]. A higher filter cut off frequency resulted in a slight increase in MAPO since more frequency content was included. The cycle-to-cycle variation in MAPO exceeded the MAPO offset originating from sampling frequency. Therefore, the sampling frequency of 36 kHz was deemed acceptable for the analysis of MAPO knock intensity in this study. All reported MAPO values in *Section 4 Lambda Sweeps* were assessed using the 36 kHz sampling frequency and averaged across 300 consecutive cycles.

Because of common concerns about indicating spark plugs, an uncooled 2mm recessed Kistler 6044A pressure transducer was installed in the knockmeter port and replaced the standard D1 pickup for a standard PRF98 test. The MAPO knock intensities of the indicating spark plug and the Kistler 6044A were within ±0.1 bar, with slightly lower MAPO readings for the Kistler transducer (Table 6). This is presumably due to the Kistler 6044A pressure transducer being mounted perpendicular to the knocking pressure waves, while the side-mounted spark plug pressure transducer was mounted in line with the knocking pressure oscillations. Again, the MAPO offset due to a lower filter cut off frequency of 18 kHz instead of 40 kHz was within the cycle-to-cycle MAPO variation.

Table 6. Validation of sampling frequency and transducer type for MAPO calculation.

High Frequency Cut-Off [kHz]	**AVL GU13Z-24 indicating spark plug**		**Kistler 6044A in knockmeter port**	
	MAPO Average [bar]	**Cycle-to-cycle MAPO standard deviation [bar]**	**MAPO Average [bar]**	**Cycle-to-cycle MAPO standard deviation [bar]**
18 kHz	0.69	± 0.21	0.63	± 0.17
40 kHz	0.79	± 0.23	0.67	± 0.18

At standard RON conditions, every cycle was knocking and the cyclic variation of knock intensity was low, making the 300 cycle averaged MAPO knock intensity measurements very representative and repeatable. However, to determine a minimum MAPO threshold for data analysis, an experiment was conducted at a retarded spark timing (20°aTDC) compared to the standard RON test to reduce the knock intensity and create stochastic knock from cycle to cycle, shown in Figure 4A. While testing with a retarded spark timing, only three of the 300 combustion cycles (47, 100, 115) showed a MAPO value beyond the signal noise. Figure 4B shows the cylinder pressure and the bandpass filtered knock signal for cycles 47, 100, and 115. Cycle 47 showed the highest maximum amplitude of pressure oscillations and the start of pressure oscillations follows a similar behavior as shown in Figure 3 which clearly characterized knocking combustion. Of the three cycles, Cycle 100 had the lowest MAPO reading and no clear oscillation due to knocking combustion is visible. Cycle 115 showed a borderline case with pressure oscillations slightly beyond the signal noise floor. While this could be characterized as knocking combustion, the intensity is deemed too low and no oscillations are visible for the cylinder pressure. Based on this analysis, a MAPO value of 0.1 bar was selected as a knock threshold to determine the difference between knocking and non-knocking cycles in this work.

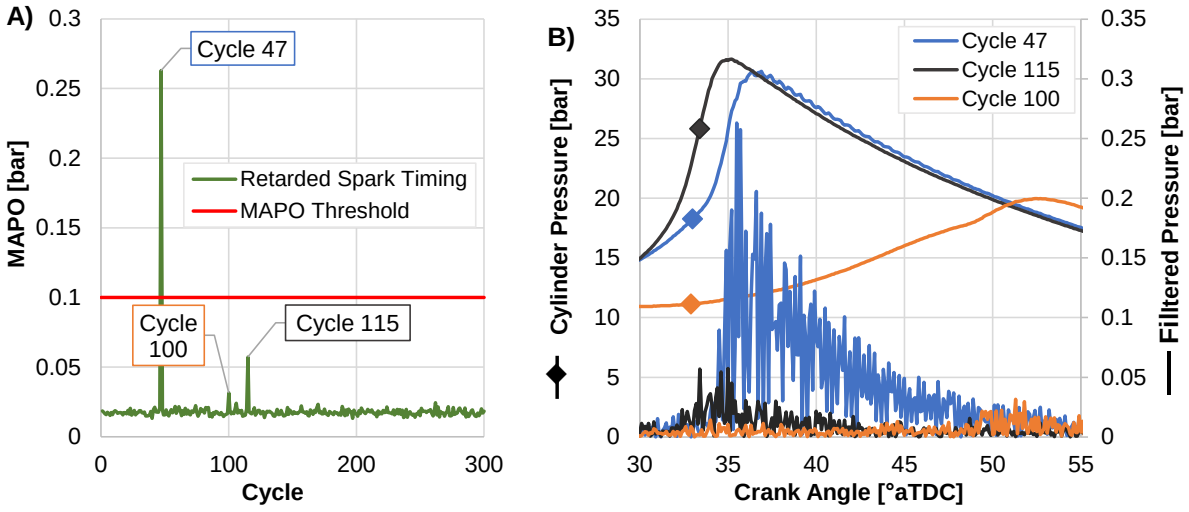

275

276 *Figure 4.A) Cyclic MAPO values with three stochastic knock events and their respective pressure trace.*

277 *B) Respective pressure traces and bandpass filtered knock signal for three stochastic cycles*

278 Figure 5 shows a 300 cycle MAPO distribution for standard and stoichiometric RON conditions for PRF95
279 and fuels with the lowest MAPO knock intensities (PRF97, TSF96.9, and the lowest MAPO knock intensity
280 FACE fuels FACE B and FACE G). For standard RON operating conditions (standard compression ratio, spark
281 timing, and peak knocking lambda), almost all cycles exceeded the set MAPO knock threshold of 0.1 bar,
282 Figure 5A. It is noted, that cycles with a MAPO value exceeding 1.1 bar are shown in an overflow bin in
283 Figure 5A to focus on the low-knocking cycles. Only TSF96.9 had 13 cycles with a MAPO knock intensity
284 below 0.1 bar which is due to its high RON of 96.9 compared to the set compression ratio for a RON 95
285 gasoline. The FACE G also showed two cycles with non-knocking cycles which goes along with its high
286 measured RON of 96.5 (compare Table 7). Lambda conditions outside of the peak knocking lambda, such
287 as at stoichiometry, cause a reduced knock intensity, Figure 5B. Despite reducing the knock intensity by
288 operating the engine at stoichiometry, all FACE fuels and PRF95 had knocking combustion for most of the
289 300 cycles. Even the higher RON PRF97, which was also tested at the compression ratio setting for RON
290 95 fuels, still exceeded the 0.1 bar MAPO threshold for 93% of the combustion cycles. In addition, the
291 ensemble-averaged MAPO correlates with the two most prominent MAPO ranges. This allowed the

authors to compare fuels between their standard RON peak knocking lambda and non-standard stoichiometric tests based on an ensemble-averaged MAPO value of all 300 combustion cycles.

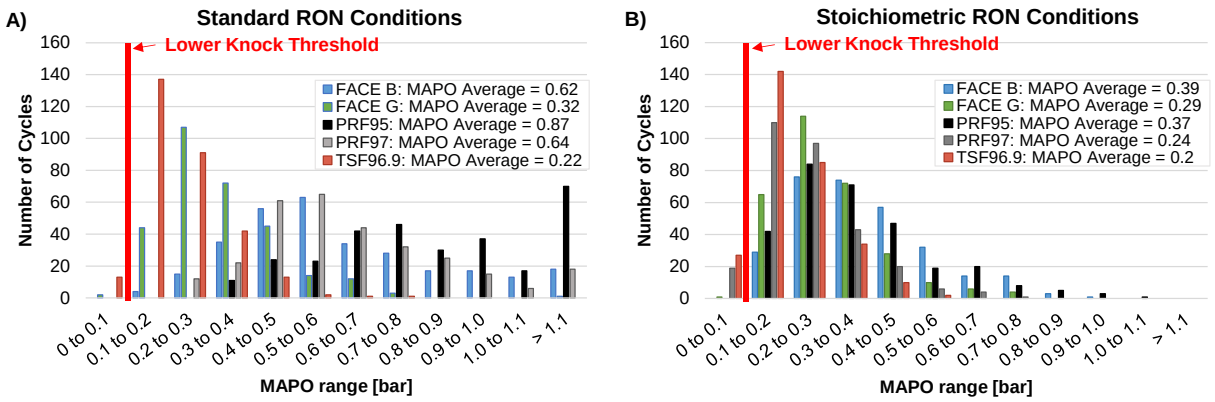

Figure 5. Cyclic MAPO distribution and MAPO average of combustion cycles at standard RON (A) and stoichiometric RON (B) conditions. Figure 5A shows existing cycles with MAPO values exceeding 1.1 in an overflow bin.

4. Lambda Sweeps

Lambda sweeps from 0.8 to 1.0 were performed for all tested fuels and the knock intensities, both knockmeter and cylinder pressure transducer-based, were recorded. All tests were performed at a constant compression ratio for a RON 95 fuel based on ASTM D2699 [5]. This best suited all sample fuels, which were chosen to have a RON of approximately 95. Figure 6 shows the knockmeter and pressure oscillation-based knock intensity response for PRF93, PRF95, and PRF97. Independent of the knock intensity measurement technique, a lower RON PRF resulted in a higher knock intensity. Each of the PRFs reached their maximum knock intensity at a lambda of around 0.87 – 0.89 for either knock intensity technique. A knockmeter calibration of 12 to 15 knock units per octane number is required by the standard RON test method to achieve good resolution while staying within the linearity range of the

knockmeter scale. The CFR engine manual reports the knockmeter to be linear in a range from 20 to 80 knock units, but a previous study by the authors found the knockmeter scale to be linear in a range between 10 and 90 knock units [16, 21]. The knockmeter knock intensity measurement of PRF97 at stoichiometry was lower than the linearity range of the knockmeter and couldn't be used for further analysis, while the MAPO knock intensity measurement was still above the 0.1 bar MAPO threshold.

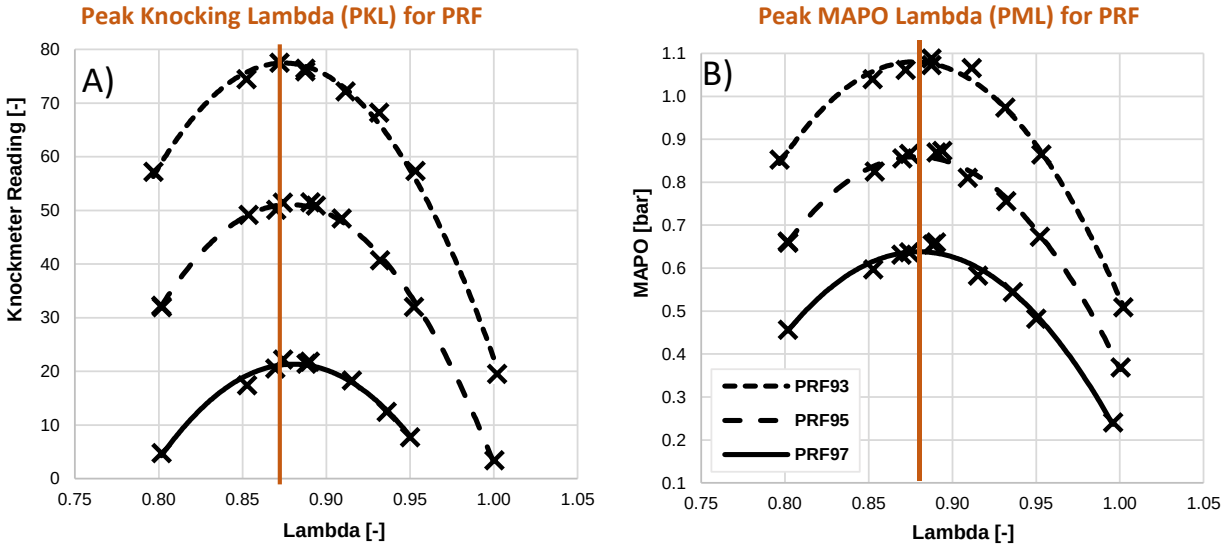

Figure 6. Knockmeter (A)- and pressure oscillation-based (B) knock intensity as a function of lambda for PRF93, 95, and 97.

Outside of the peak knocking lambda conditions, the knock intensities followed a second-order parabolic shape. This resulted in knock intensity (by both techniques) being very sensitive to small changes in lambda near stoichiometry. Figure 7 shows the knock intensity response for small changes in lambda around stoichiometry for PRF93 at an increased compression ratio. Changes in lambda by as little as 0.02 caused changes of 0.1 bar for the MAPO-based knock intensity and 10 knock units in the knockmeter reading. These are large offsets considering the knock intensity differences between PRF93 and PRF95 in Figure 6. The standard deviation of lambda over a measurement period of 60 seconds at steady-state conditions was ±0.015, which resulted in a coefficient of variation of 1.5%. This variation in lambda was of significant impact at stoichiometric conditions, where the knock intensity was more sensitive to

changes in lambda than at the peak knock lambda. These observations should be considered for knock studies near stoichiometry which would require improved lambda control.

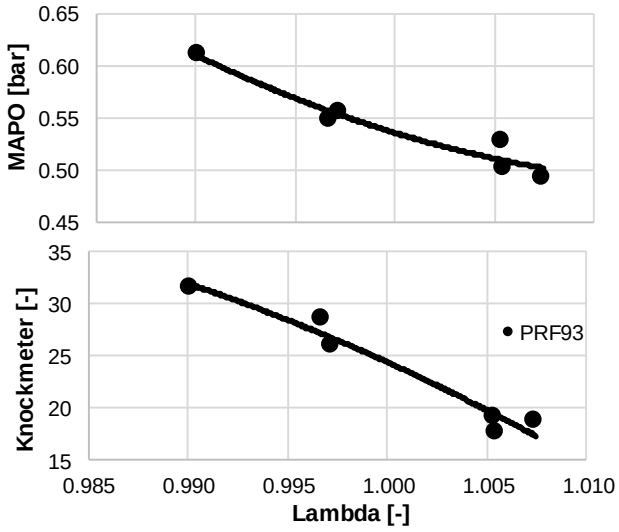

Figure 7. Knock intensity response for small variations in lambda near stoichiometric conditions for PRF93.

Figure 8A through D show the knock intensity responses to lambda for each of the seven FACE fuels in comparison to the previously discussed PRFs. The left column (A and C) depicts the knockmeter-based knock intensities, while the right set of graphs (B and D) contain the pressure-based knock intensities. The scaling of the MAPO reading from Figure 6 was modified to provide a higher resolution for the FACE fuels, which generally showed a significantly reduced MAPO-based knock intensity compared to the PRFs. The significantly higher pressure oscillations for the paraffinic PRFs were previously noted by the authors and other studies [7, 15, 16, 23, 28].

Figure 8A and B compare the knock intensities of mainly iso-paraffinic FACE gasolines to the PRFs. All FACE gasolines had a peak knockmeter reading between those of PRF93 and PRF97. The higher the peak knock intensity, the lower the RON rating of the sample fuel. An overview of the calculated RON values is provided in Table 7. The chemical composition caused a shift in the lambda of peak knock compared to the PRFs (0.90 and 0.89, respectively). FACE B is mostly iso-paraffinic and showed a PKL and peak MAPO

lambda (PML) closest to that of the PRFs. Despite the lowest peak knockmeter reading among the highly iso-paraffinic gasolines (Figure 8A) and therefore highest RON rating, FACE B showed the second-highest MAPO-based peak knock intensity (Figure 8B). This confirmed that mainly iso-paraffinic fuels lead to higher knocking cylinder pressure oscillations compared to fuels with similar RON but lower iso-paraffinic content as shown in previous studies [7, 16, 28]. The closest PKL and PML to stoichiometry among the highly iso-paraffinic fuels was seen for FACE F (0.93 and 0.95, respectively), which had high concentrations of olefins and cycloparaffins. Adding ethanol shifted the PKL and PML towards stoichiometry, as was the case for FACE A (0.94 and 0.93, respectively) and FACE C (0.93 and 0.95, respectively), similar to those of FACE F.

Figure 8C and D show the lambda sweeps for mainly aromatic FACE gasolines, which generally showed a PKL and PML closer to stoichiometry compared to mainly iso-paraffinic fuels (FACE D compared to FACE B). Added olefins and cycloparaffins (FACE G) again shifted the PKL and PML towards stoichiometry, which validated the previously noted trend for FACE F. No additional shift in PML or PKL was noted for FACE H, which represents a highly aromatic fuel with added olefins, cycloparaffins, and ethanol. While FACE D still showed similarities to the parabolic knock intensity curves of PRFs, FACE G and H show significantly reduced knock intensities at rich conditions. These analyses showed that none of the gasolines or PRFs generated their peak knock intensity at stoichiometry, and all of them were generated at slightly rich lambda conditions.

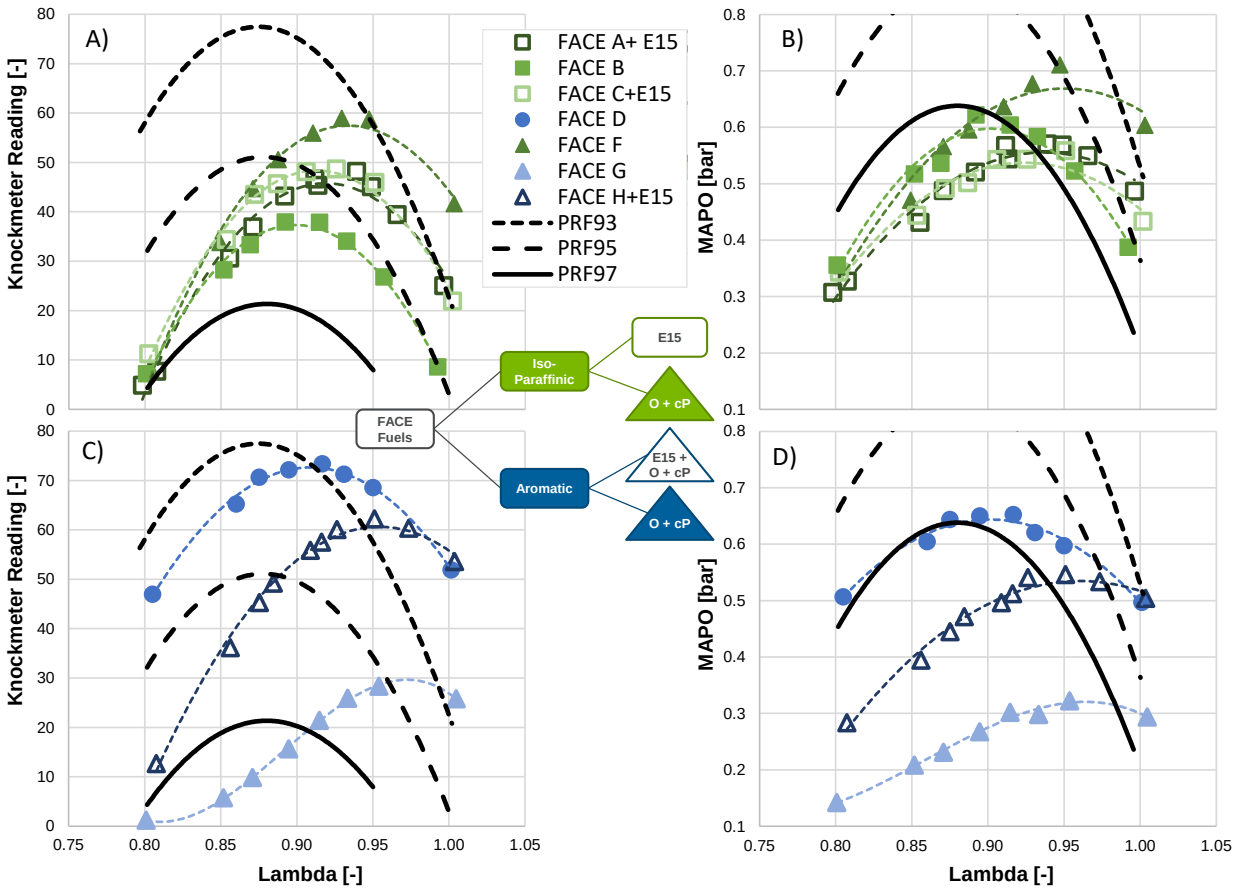

Figure 8. Knockmeter- (A and C) and cylinder pressure oscillation-based (B and D) knock intensity as a function of lambda for FACE gasolines and bracketing PRFs.

5. Standard RON Test Results

The RON values of the FACE gasolines were calculated using Equation 2 at their peak knock lambda and are summarized in Table 7. Table 7 also compares the RON ratings measured in this work to those described in CRC report AVFL-24 [20]. An overview of the peak knockmeter lambda, peak MAPO lambda, and peak MAPO knock intensity measured during standard RON rating are also shown. All RON ratings of the FACE fuels in this work were within the ASTM reproducibility limit of ±0.7 RON from those published

in the CRC AVFL-24 report [5]. It was noticed that all but one fuel rated higher than expected. FACE D showed a -0.7 ON offset in RON rating compared to positive offsets for the other FACE fuels. Table 7 shows that the lambda of peak knockmeter reading and lambda of peak MAPO reading closely correlated within ±0.01 lambda. The peak MAPO values are reported as well. It can be seen that FACE G, a fuel with high aromatic, cyclo-paraffin, and olefin content, had the lowest MAPO while also having the highest RON. However, this was not true for all blends. For example, FACE B had the second-highest RON of the test fuels while also having a higher MAPO than FACE A, C, and H, which all contained 15 vol% ethanol. Based on Figure 8, it was previously described that PRFs had a noticeably higher MAPO for their RON level.

Table 7. Overview of RON ratings and lambda of both, peak knockmeter reading and peak MAPO under standard RON test conditions for each FACE gasoline and reference fuels.

FACE Fuel	Current RON	Previous RON [20]	Current - Previous RON Offset	Peak Knockmeter Lambda	Peak MAPO Lambda	Peak Knockmeter Reading	Peak MAPO [bar]
B	95.9	95.8	0.1	0.90	0.89	37.9	0.62
D	93.5	94.2	-0.7	0.92	0.90	73.4	0.65
F	94.5	94.0	0.5	0.93	0.95	58.9	0.71
G	96.7	96.5	0.2	0.95	0.95	28.3	0.32
A + E15	95.2	94.8	0.4	0.94	0.93	48.1	0.57
C + E15	95.2	94.8	0.4	0.93	0.95	48.6	0.56
H + E15	94.3	94.1	0.2	0.95	0.95	62.2	0.55
PRF97	97	N/A	N/A	0.88	0.88	23.0	0.65
PRF95	95	N/A	N/A	0.88	0.88	52.8	0.90
PRF93	93	N/A	N/A	0.88	0.88	76.1	1.12
TSF96.9	97.2	N/A	N/A	0.93	0.93	20.2	0.22
TSF93.4	93.7	N/A	N/A	0.93	0.93	67.3	0.43

5.1. Effects of Lambda and Knock Intensity Metric on the Effective RON Ratings

The previously discussed standard RON ratings were calculated based on the knockmeter at the lambda that gave the peak knock intensity following the ASTM D2699 method [5]. Any of the following conditions with operating parameters outside of the standard RON are not official RON ratings but rather effective RON calculations.

Figure 9 shows the knockmeter and MAPO response to a lambda sweep for each of the FACE gasolines and for the bracketing PRFs. For an effective RON calculation at a given lambda, i.e. stoichiometry, the knock intensity of the FACE fuels changed relative to the bracketing PRFs. The three tested PRFs created two interpolation zones as graphically highlighted in Figure 9. Ideally, all FACE fuels would be bracketed by PRFs, but due to the differing knock intensity response to lambda between fuels, the two interpolation zones spanning between PRF97, PRF95, and PRF93 did not cover all collected data points across the full lambda sweep.

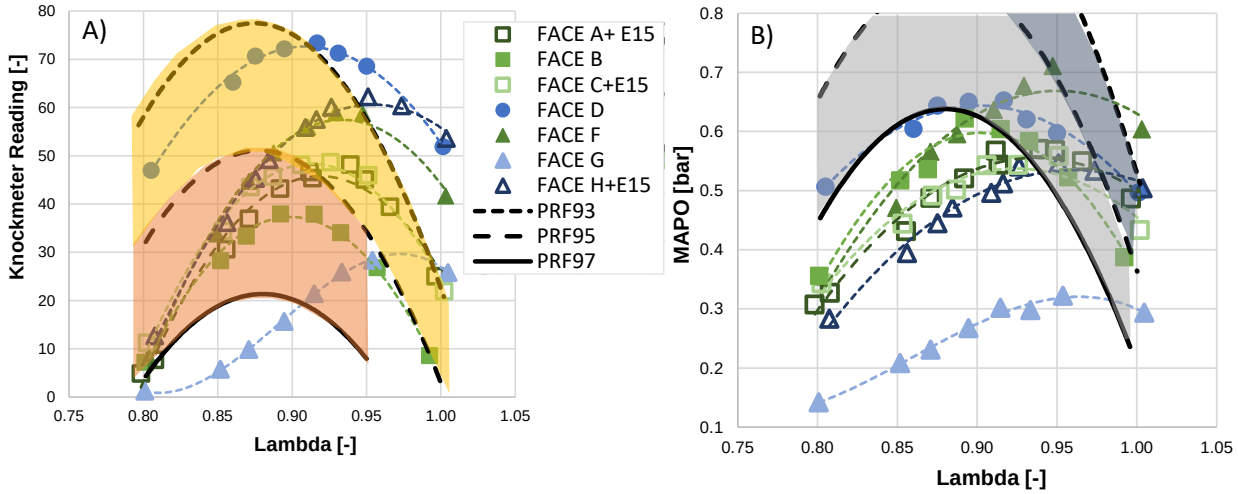

Figure 9. Knockmeter- (A) and pressure oscillation-based (B) knock intensities for FACE gasolines with highlighted interpolation areas between PRFs.

The standard RON rating of each FACE gasoline was assessed based on Equation 2 at the lambda of highest knockmeter reading. It is also possible to substitute the MAPO-based knock intensity and calculate a MAPO-based RON rating, which was introduced in a previous publication by the authors and was applied in this study [16]. To calculate the variation in RON rating across the lambda sweep, the knock intensity of the sample fuel was compared to the knock intensity of the bracketing PRFs at the same lambda. Note that by definition, the effective RON value of the PRFs would be the same as their iso-octane concentration at each lambda, denoted by the black lines in Figure 10. Generally, the RON ratings based on MAPO, displayed in Figure 10B, exceeded those of the knockmeter based RON calculation from Figure 10A. This was due to the relatively higher MAPO knock intensity of PRFs, as shown in Figure 8 and Figure 9. Any equivalent RON value beyond RON 97 or below RON 93 was extrapolated based on PRF97 and PRF95, or PRF95 and PRF93. For rich conditions lower than lambda of 0.9, most FACE fuels exceeded their standard RON rating and were more knock resistant compared to PRFs (Figure 10B). When shifting towards stoichiometric operating conditions, the RON ratings of the FACE fuels decreased sharply. The knockmeter-based RON rating of the fuels dropped below RON 93. The MAPO-based stoichiometric RON ratings of the FACE fuels were mostly in the range of RON 97 to RON 95. Therefore, when rated based on pressure oscillations, the FACE fuels at stoichiometric conditions coincidentally returned somewhat close to their ASTM RON rating.

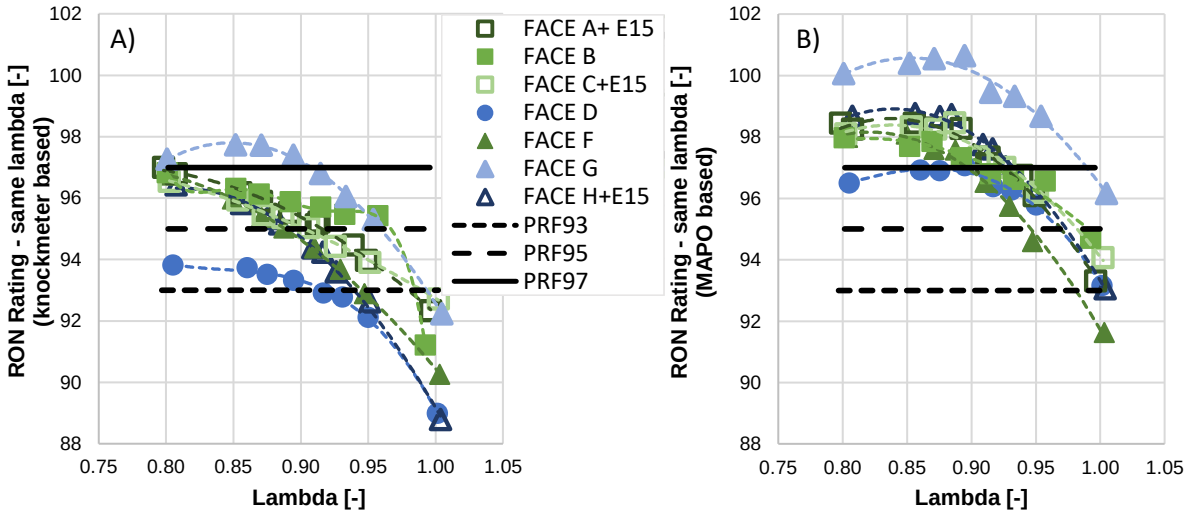

413

414 *Figure 10. Effects of lambda and knock intensity metric on RON ratings of the FACE gasolines.*

415 The RON ratings at stoichiometry are summarized and compared to their standard ASTM RON ratings in
416 Figure 11. The standard ASTM RON ratings are shown with error bars representing the repeatability limit
417 of ±0.2 RON of the ASTM testing procedure, while the error bars for the stoichiometric RON calculations
418 are based on the previous discussion of the lambda uncertainty from Figure 7 [5]. This resulted in a
419 measurement uncertainty of ±1.25 RON for both knockmeter and MAPO-based RON calculations at
420 stoichiometry. The ASTM repeatability is based on a statistical analysis of extensive inter-laboratory
421 studies while the measurement uncertainty at stoichiometry is a measurement uncertainty based on
422 lambda control, hence both uncertainties describe different aspects. The stoichiometric RON ratings
423 based on the knockmeter were significantly less than the standard ASTM RON ratings, by 2 - 5 RON. The
424 MAPO-based stoichiometric RON ratings, however, were more close to the standard RON ratings, and
425 within 0.5 - 2.5 RON. A systematic offset towards lower RON levels was noted for any of the stoichiometric
426 RON ratings compared to the standard ASTM RON ratings. When taking measurement uncertainty at
427 stoichiometry into account, two of the seven FACE fuels' MAPO-based stoichiometric RON ratings (FACE
428 F and A+E15) were at or outside the measurement uncertainty compared to their standard RON ratings.
429 Both fuels are characterized as being highly isoparaffinic. All predominantly aromatic FACE gasolines (FACE

D, G, and H+E15) had a MAPO-based stoichiometric RON rating within the stoichiometric measurement uncertainty to their standard RON rating. A study by Shah et al. on a modern single-cylinder SI engine found an improved correlation between the knock-limited spark advance ratings of several RON 98 gasolines and their MAPO-based stoichiometric RON ratings compared to their standard RON ratings [29].

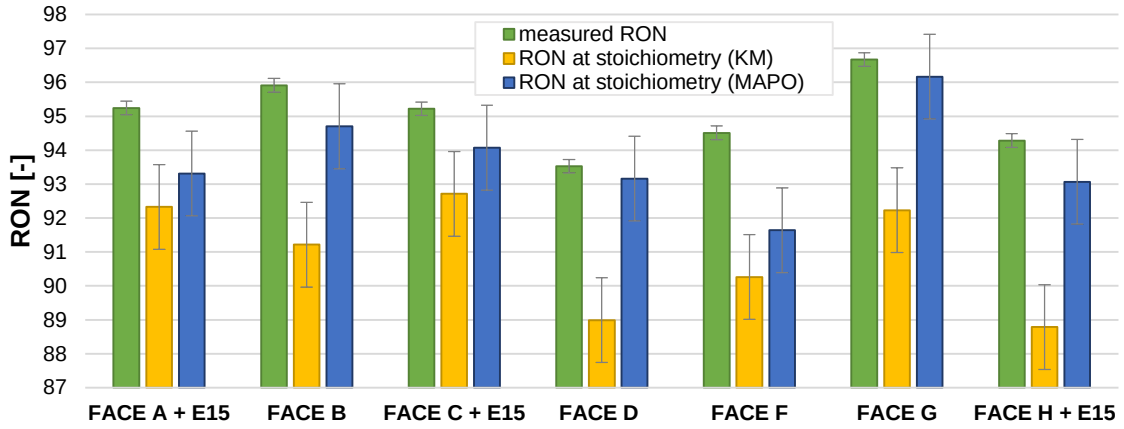

Figure 11. Overview of RON ratings for FACE fuels at stoichiometry compared to their standard RON value. The error bars represent the repeatability for the measured RON rating and the measurement uncertainty for effective RON ratings at stoichiometry.

5.2. Correlation between Octane and MAPO

The following correlations are quantitatively evaluated based on the coefficient of determination (R^2) of a linear regression which describes the relation between two parameters ranging from no correlation ($R^2 = 0$) to perfect correlation ($R^2 = 1$).

The effect of fuel chemistry on pressure-based knock intensity (MAPO) is analyzed in Figure 12 for PRFs, TSFs, and FACE fuels in comparison to their standard ASTM RON ratings. The MAPO values were assessed while performing the standard RON test at the lambda of peak knockmeter knock intensity. The overall correlation of MAPO to standard RON ratings for all fuels (solid black line in Figure 12) was very low ($R^2 = 0.29$). Generally, PRFs showed the highest MAPO knock intensities of all fuels, while TSFs had the lowest.

447 Plotting regression lines for fuels that belong to certain chemical families, such as PRFs (black dashed),
448 paraffinic FACE gasolines (green dashed), aromatic FACE fuels (blue dashed), and TSFs (red dashed)
449 showed the effects of fuel chemical composition. Within a given grouping of fuel chemistry, the MAPO
450 knock intensity generally decreased with increasing RON values. The coefficient of determination for the
451 linear regression of paraffinic FACE fuels (green symbols) was much lower than the overall correlation,
452 caused in part by the small range of RON values for those fuels, and also by the effects of two fuels
453 containing 15 vol% ethanol (hollow symbols). Previous work by the authors found that the MAPO knock
454 intensities of highly paraffinic fuels are much more sensitive to small additions of ethanol than highly
455 aromatic base fuels [28]. Nevertheless, a distinct order of fuel MAPO-based knock intensities based on
456 their chemical composition was found. The PRFs and TSFs bracketed all tested gasolines, as having the
457 highest paraffinic and aromatic content, respectively. Of the FACE gasolines (which all had a standard RON
458 rating of approximately 95), mainly aromatic fuels showed consistently lower MAPO compared to highly
459 paraffinic blends. This means that when operating these fuels on an automotive engine, fuels with higher
460 aromatic or ethanol content would be more knock resistant than highly iso-paraffinic fuels with the same
461 RON.

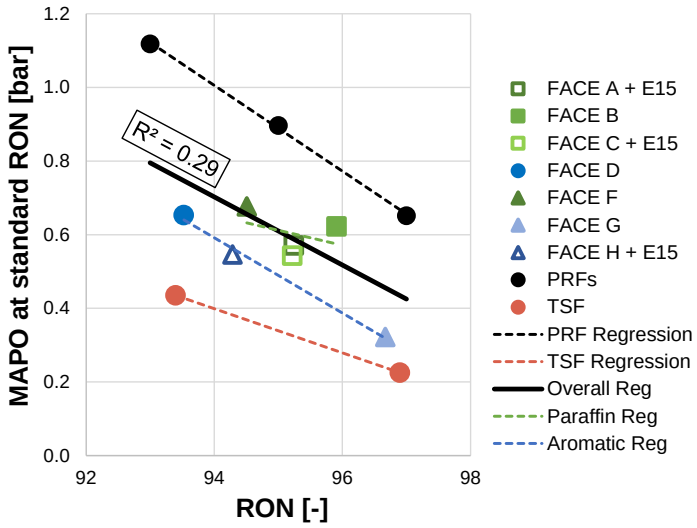

Figure 12. Correlation of MAPO and standard RON ratings for PRFs, TSFs, and FACE gasolines at standard RON conditions with linear regression lines for each chemical family.

The standard RON ratings of the tested fuels generally did not agree with their MAPO knock intensities at RON test conditions (overall regression line in Figure 12), which is consistent with previous findings by the authors [16]. The Octane Index (OI) proposed by Kalghatgi was displayed in Equation 1 [9]. Octane Index takes an engine operation factor K into account, which can be varied to achieve the best possible linear regression between the fuels' RON and MON values and some performance parameter. Typically in the literature, OI is correlated to the knock-limited spark advance for each of the fuels at a given engine operating condition. In this work, the correlation between MAPO and Octane Index for standard RON operating conditions and for stoichiometric operation is explored (Figure 13A and B). The K factor for best correlation is displayed on the graphs along with the coefficient of determination (R^2). Figure 13A contains the MAPO knock intensity from the standard RON test at peak knocking lambda (PKL) for the three bracketing PRFs, two TSFs, and seven FACE gasolines. This takes into account the high-frequency components of knock, more similar to how knock would be measured on an automotive engine by a cylinder pressure transducer or knock sensor. While Figure 12 showed a poor correlation between MAPO and standard RON, there was a high correlation between MAPO and Octane Index in Figure 13A at each

fuel's PKL for a K factor of K = -0.48. Despite all fuels in Figure 13A being tested at standard RON operating conditions, the negative K value suggests the engine operating conditions were at "beyond RON" conditions (K<0) when using a MAPO knock intensity rather than the standard CFR knockmeter. This effect resulted solely from the change of the knock intensity measurement technique from the CFR knockmeter to MAPO, while at standard RON conditions (spark timing, compression ratio, lambda of peak knock intensity, etc.). When comparing Figure 12 with Figure 13A, it can be seen that the Octane Index of PRFs was identical to their RON values due to PRFs having zero octane sensitivity. All other fuels, which have a RON-MON sensitivity above zero, had a higher Octane Index than their standard RON values due to the negative K factor. Therefore, higher octane sensitivity was beneficial for the MAPO-based knock resistance of the fuel at standard RON test conditions.

Figure 13B shows the correlation between MAPO and Octane Index with the CFR engine operated at stoichiometric conditions, which lead to a reasonably acceptable correlation of R^2 = 0.73 for a K value slightly above zero. This analysis would more closely replicate the knock test conditions on an automotive engine (stoichiometric conditions and MAPO-based knock intensity). Previous studies have shown, that stoichiometric conditions typically lead to an increased K-value compared to rich conditions [9, 10, 12]. The pressure oscillation-based knock intensity correlated reasonably well with Octane Index at stoichiometric conditions with a K value near zero which represents the standard RON test (at peak knocking lambda). A similar result was observed in Figure 11 when the MAPO-based RON at stoichiometry correlated closer to the standard RON of the fuel than at stoichiometry with the knockmeter. This could be an indicator of why RON as a fuel property still reasonably characterizes the fuel's anti-knock performance in automotive engines operating at stoichiometry and with knock intensity characterized by the high-frequency knock content. In Figure 13B, it can also be seen that mainly paraffinic FACE fuels typically showed higher pressure oscillation based knock intensities than the regression line, whereas

mainly aromatic FACE fuels caused lower pressure oscillation based knock intensities. Stoichiometric data for both TSFs were not taken during this campaign.

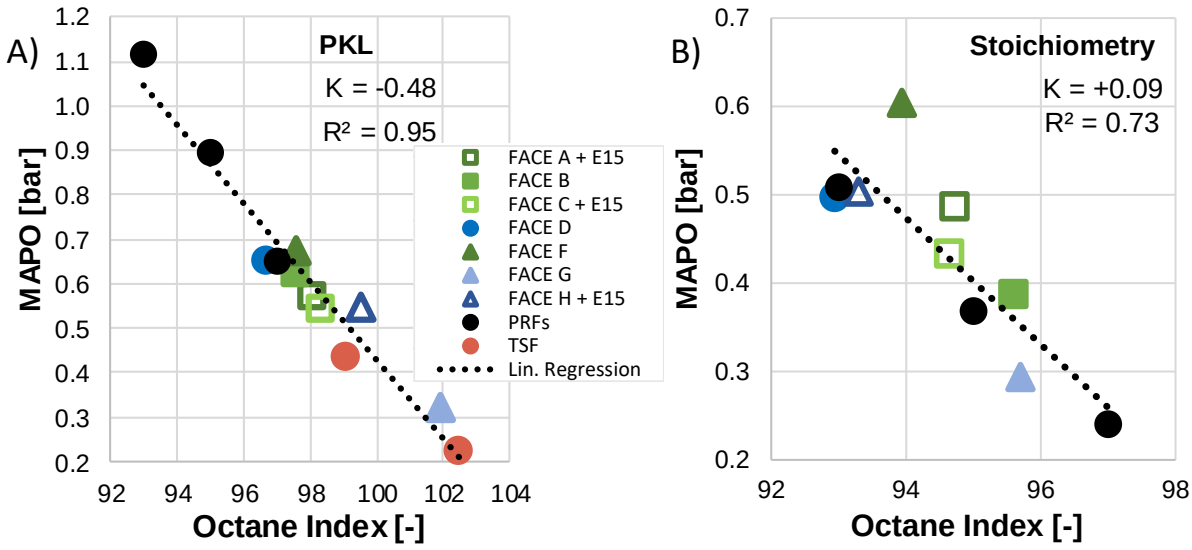

Figure 13. Correlation of MAPO to Octane Index for PRFs, TSFs, and FACE gasolines at standard RON test conditions (PKL (A)) and stoichiometric conditions (B).

6. Summary

The observations of this work can be summarized as follows:

- The seven CRC FACE gasolines with approximately RON 95 were characterized into mainly paraffinic or aromatic fuels, each having ethanol and/or cycloparaffins and olefins added to some of the fuels.
- The knockmeter 501C detonation meter filtered out knocking pressure oscillations, which caused RON not to correlate to a pressure-oscillation based knock intensity (MAPO). A sampling rate of

36 kHz and the use of the spark plug pressure transducer proved sufficient to characterize the pressure oscillation-based knock intensity on the CFR engine under RON test conditions.

- For standard RON conditions at a compression ratio level of RON 95, each cycle was knocking when applying a MAPO knock intensity threshold of 0.1 bar. At the compression ratio for RON 95 fuels and stoichiometric conditions, RON 97 fuels still had more than 90% of the cycles knocking.

- The lambda of peak knockmeter and peak MAPO knock intensity closely correlated under RON test conditions. Paraffinic fuels showed the richest peak knock lambda. Ethanol, aromatics, cycloparaffins, and olefins shifted the lambda of peak knock towards stoichiometry. The parabolic knock intensity response to changes in lambda caused a high knock intensity sensitivity to small changes in lambda at stoichiometric conditions.

- The tested PRFs showed significantly higher MAPO-based knock intensities compared to TSFs and FACE gasolines at the same test conditions. Paraffinic components generally showed higher knocking pressure oscillations compared to aromatic fuels. Within a chemical family, a higher RON resulted in lower pressure oscillations.

- The measured RON values in this testing showed good agreement within the reproducibility range compared to the values in CRC report AVFL-24. The MAPO-based RON at a given lambda was generally higher compared to the knockmeter-based RON because of the high MAPO behavior of PRFs. Both knock intensity-based RON calculations decreased towards stoichiometry, which resulted in coincidentally better agreement between the MAPO-based RON at stoichiometry and the standard RON of the FACE fuels, but a worse correlation with the knockmeter-based RON at stoichiometry.

- At standard RON conditions (at peak knocking lambda), a K factor of K = -0.48 showed the best correlation between a pressure oscillation-based knock intensity (MAPO), which is typically used

on automotive engines, and Octane Index. For stoichiometric conditions, a K factor of K = 0.1 caused the best correlation between MAPO and Octane Index.

The findings from this first part of the three-part publication series advocate a continued investigation into the differences between how the ASTM RON test method rates knock resistance of fuels compared to best practices on modern automotive SI engines. The next parameters to be considered include knock-limited spark advance methods (part two) and variations in knock limited compression ratio (part three). The test conditions will focus on stoichiometric RON operation using MAPO-knock intensity and PKL operation for both MAPO and knockmeter knock intensity measurements.

7. Acknowledgments

The authors would like to thank the Coordinating Research Council (CRC) task group Advanced Vehicle Fuel Lubricants AVFL-32 for providing the FACE fuels, funding, and project guidance.

The authors would also like to thank Stephan Schneider for his assistance during the experimental work and Timothy Rutter for his technical support.

Argonne is a U.S. Department of Energy laboratory managed by UChicago Argonne, LLC under contract DE-AC02-06CH11357.

8. References

1. Heywood, J., “Internal Combustion Engine Fundamentals,” New York: McGraw-Hill, 1998. ISBN: 0-07-028637-X
2. ASTM D4814-18a, “Standard Specification for Automotive Spark-Ignition Engine Fuel,” ASTM International, West Conshohocken, PA, 2016, doi: 10.1520/D4814-18A
3. EN 228, “Automotive Fuels – Unleaded petrol – Requirements and Test Methods,” German Version EN228:2012+A1:2017. Deutsches Institut für Normung, August 2017.
4. Japanese Standards Association, “Motor Gasoline – JIS K 2202”, 2012.
5. ASTM D2699-15a, “Standard Test Method for Research Octane Number of Spark-Ignition Engine Fuel,” ASTM International, West Conshohocken, PA, 2015, doi: 10.1520/D2699-15A
6. ASTM D2700-16, “ Standard Test Method for Motor Octane Number of Spark-Ignition Engine Fuel,” ASTM International, West Conshohocken, PA, 2016, doi: 10.1520/D2400-16
7. Swarts, A., Yates, A., Viljoen, C., and Coetzer, R., "A Further Study of Inconsistencies between Autoignition and Knock Intensity in the CFR Octane Rating Engine," SAE Technical Paper 2005-01-2081, 2005, doi:10.4271/2005-01-2081.
8. Yates, A., Swarts, A., and Viljoen, C., "Correlating Auto-Ignition Delays And Knock-Limited Spark-Advance Data For Different Types Of Fuel," SAE Technical Paper 2005-01-2083, 2005, doi:10.4271/2005-01-2083.
9. Kalghatgi, G., "Fuel Anti-Knock Quality - Part I. Engine Studies," SAE Technical Paper 2001-01-3584, 2001, doi:10.4271/2001-01-3584.

10. Mittal, V. and Heywood, J., "The Shift in Relevance of Fuel RON and MON to Knock Onset in Modern SI Engines Over the Last 70 Years," SAE Int. J. Engines 2(2):1-10, 2010, doi:10.4271/2009-01-2622.
11. J. Szybist, D. Splitter, "Understanding chemistry-specific fuel differences at a constant RON in a boosted SI engine", Fuel, Volume 217, 2018, Pages 370-381, doi:10.1016/j.fuel.2017.12.100.
12. Mittal, V. and Heywood, J., "The Relevance of Fuel RON and MON to Knock Onset in Modern SI Engines," SAE Technical Paper 2008-01-2414, 2008, doi:10.4271/2008-01-2414.
13. Hunwartzen, I., "Modification of CFR Test Engine Unit to Determine Octane Numbers of Pure Alcohols and Gasoline-Alcohol Blends," SAE Technical Paper 820002, 1982, https://doi.org/10.4271/820002.
14. Foong, T., Morganti, K., Brear, M., da Silva, G. et al., "The Effect of Charge Cooling on the RON of Ethanol/Gasoline Blends," SAE Int. J. Fuels Lubr. 6(1):34-43, 2013, doi:10.4271/2013-01-0886.
15. Hauber, J., Huber, K., and Nell, R., "New GKI - Gasoline Knock Index for Rating of Fuel's Knock Resistance on an Upgraded CFR Test Engine," SAE Technical Paper 2018-01-1743, 2018.
16. Hoth, A., Pulpeiro Gonzalez, J., Kolodziej, C., and Rockstroh, T., "Effects of Lambda on Knocking Characteristics and RON Rating," SAE Int. J. Adv. & Curr. Prac. in Mobility 1(3):1188-1201, 2019, https://doi.org/10.4271/2019-01-0627.
17. Foong, T., Brear, M., Morganti, K., et al., "Modeling End-Gas Autoignition of Ethanol/Gasoline Blends in the Cooperative Fuel Research Engine," Energy Fuels 2017, 31, 3, 2378 – 2389, December 15, 2016.
18. Pitz, W., Cernansky, N., Dryer, F., Egolfopoulos, F. et al., "Development of an Experimental Database and Chemical Kinetic Models for Surrogate Gasoline Fuels," SAE Technical Paper 2007-01-0175, 2007, https://doi.org/10.4271/2007-01-0175.

19. Sarathy, M., Farooq, A., Kalghatgi, G., “Recent progress in gasoline surrogate fuels”, Progress in Energy and Combustion Science, Volume 65, 2018, Pages 67 – 108, doi:10.1016/j.pecs.2017.09.004
20. Cannella, W., Foster, M., Gunter, G., et al., “FACE Gasolines and Blends with Ethanol: Detailed Characterization of Physical and Chemical Properties”, CRC Report No. AVFL-24, 2014.
21. Waukesha CFR, “F-1 & F-2 Research Method (F-1) Motor Method (F-2) Octane Rating Units Operation & Maintenance”, Second Edition, 2003.
22. Swarts, A. and Yates, A., "Insights into the Role of Autoignition during Octane Rating," SAE Technical Paper 2007-01-0008, 2007, doi.org/10.4271/2007-01-0008.
23. Swarts, A., Anderson, G., and Wallace, J., "Comparing Knock between the CFR Engine and a Single Cylinder Research Engine," SAE Technical Paper 2019-01-2156, 2019.
24. Huber, K., Hauber, J., Raba, A., and Nell, R., “New Test Procedure to Determine Fuel’s Knock Resistance,” MTZ-Motortechnische Zeitschrift 74(7/8):62-69, 2013.
25. Swarts, A. and Kalaskar, V., “Bridging the Knock Severity Gap to CFR Octane Rating Engines,” SAE Technical Paper 2020-01-2050, 2020.
26. Rockstroh, T., Kolodziej, C., Jespersen, M., et al., "Insights into Engine Knock: Comparison of Knock Metrics across Ranges of Intake Temperature and Pressure in the CFR Engine," SAE Technical Paper 2018-01-0210, 2018, doi:10.4271/2018-01-0210.
27. Shahlari, A. and Ghandhi, J., "Pressure-Based Knock Measurement Issues," SAE Technical Paper 2017-01-0668, 2017, https://doi.org/10.4271/2017-01-0668.
28. Hoth, A., Kolodziej, C., Rockstroh, T. et al., “Combustion Characteristics of Match-Blended PRF and TSF Fuels with Ethanol in an Instrumented CFR Engine,” SAE Technical Paper 2018-01-1672.

29. Shah, A., Hoth, A., Kolodziej, K., Rockstroh, T., “Gasoline Fuels Properties for Multi-Mode Operation – Observations in a GDI and the CFR engine, (in review)

9. Abbreviations

AKI	Antiknock Index
ASTM	American Society for Testing and Materials
°aTDC	crank angle degree after Top Dead Center
CAD	Crank Angle Degree
CFR	Cooperative Fuel Research
CRC	Coordinating Research Council
DAQ	Data Acquisition System
FACE	Fuels for Advanced Combustion Engines
HOV	Heat of Vaporization
KLSA	Knock Limited Spark Advance
KM	Knockmeter
MAPO	Maximum Amplitude of Pressure Oscillations
MON	Motor Octane Number
OI	Octane Index
PKL	Peak Knocking Lambda
PML	Peak MAPO Lambda
PRF	Primary Reference Fuel
RON	Research Octane Number

646	S	RON-MON Sensitivity
647	SI	Spark Ignition
648	T90	90% Distillation Temperature
649	TSF	Toluene Standardization Fuel

650